KLL resonant transfer excitation to $F^{6+}(1s2l2l')$ intermediate states

D. H. Lee, P. Richard, J. M. Sanders, T. J. M. Zouros,* J. L. Shinpaugh,† and S. L. Varghese‡
J. R. Macdonald Laboratory, Department of Physics, Kansas State University, Manhattan, Kansas 66506
(Received 25 February 1991)

Resonant transfer excitation (RTE) was observed and RTE Auger-electron cross sections were measured for the formation of F^{6+} $(1s2l2l')$ states in collisions of 0.25–2 MeV/u $F^{7+}(1s^2\,{}^1S, 1s2s\,{}^3S)$ with H_2 and He at zero degrees with respect to the beam direction. The measured Auger-electron differential cross sections agreed well with a modified treatment of the usual impulse approximation and the recent angular dependence theory of RTE by Bhalla [Phys. Rev. Lett. **64**, 1103 (1990)], thus confirming the selective population of the $M_L=0$ magnetic substate in RTE processes. The extracted resonant excitation scattering strengths for the $1s2p^2\,{}^2D$ and $1s(2s2p\,{}^1P)^2P_+$ states were found to be $(35\pm2)\times10^{-19}$ and $(14\pm2)\times10^{-19}$ cm^2 eV, respectively. These two states showed the strongest *KLL* RTE signature as predicted by theory.

I. INTRODUCTION

Resonant transfer excitation [1–3] (RTE) in energetic ion-atom collisions has been studied extensively in recent years [4–20]. RTE is a two-electron process in which a weakly bound (quasifree) target electron is transferred to an orbital ($n\geq2$) of the projectile and simultaneously excites a projectile electron. The resulting doubly excited state must relax either by radiative (x-ray) decay [2,11,13,15] (RTEX) or autoionization (Auger) decay [4–12,14,18] (RTEA).

If the captured electron were truly free, RTEX and RTEA would be equivalent to dielectronic recombination [3,21] (DR) and resonant excitation scattering [3,16] (RES) in electron-ion collisions, respectively. DR is a process of fundamental interest in the high-temperature plasmas of laboratory or astrophysical environments. In particular, DR is thought to be an important energy-loss mechanism in fusion technology. DR has recently been observed in merged ion-electron beams [22], and in electron-beam ion traps [23] (EBIT) and sources [24] (EBIS). RES is analogous to the well-known resonant scattering in electron-atom collisions [25]. Since both RES and DR are deexcitation channels of the same doubly excited state, measurements of RES cross sections can complement DR cross sections.

The production mechanism of the doubly excited, intermediate state $|d\rangle$ is a correlated electron-electron interaction [26]. DR and RES, and similarly RTEX and RTEA, are resonant in electron energy in the ion rest frame. Furthermore, they should have an *angular* dependence in their deexcitation processes due to the collisional alignment of the $|d\rangle$ state, which represents the preferential population of the $M_L=0$ magnetic substate [11,12,17,18]. In addition, since the production channel of the $|d\rangle$ state is a time-reversed Auger process, the state production cross section or strength can be calculated from the Auger rate between the excited $|d\rangle$ state and the initial $|i\rangle$ state.

RTEA and RTEX cross sections have been measured and compare favorably with theory [11,15,16,19,20], mostly within the impulse approximation [15,27], from which DR or RES cross sections can be extracted. Many experimental RTEX studies [2,13], in which *K*-shell excitation ($\Delta n\geq1$ transition) is involved, have been performed for $Z\geq9$, but individual $|d\rangle$ states were not resolved due to the low resolution of the Si(Li) x-ray detector. The most stringent tests of RTE and its associated resonant strength (cross section) have been supplied by state-selective studies [5,8,9,12] for $Z=8,9$ using high-resolution Auger electron spectroscopy.

In this article, we report on RTEA and its RES strength measured at $\theta_{lab}=0°$ with respect to the projectile beam direction for $F^{6+}(1s2l2l')^{(2S+1)}L$ intermediate states formed in collisions of 0.25–2 MeV/u F^{7+} with H_2 and He targets. All the $1s2l2l'^{(2S+1)}L$ states were investigated, and their *KLL* RTEA cross sections were determined so far as their cross sections were measurable. These state-resolved cross sections showed a good agreement with theoretical calculations. The RTEA measurements for the ^2D and ^2P states, which have different total angular momentum L, complement the recent studies on the angular dependence [11,12,17,18] of RTE, in which it was shown that the angular differential cross sections of RTEA are determined by the total angular momentum L in the LS coupling scheme.

II. EXPERIMENT

This work was performed at the Kansas State University J. R. Macdonald Laboratory using an EN tandem Van de Graaff accelerator. F ions were accelerated to 4.75–38 MeV, and the beam was post-stripped with a carbon foil to achieve higher charge states. A F^{7+} beam was injected into the collision chamber after being selected by an analyzing magnet. In the production of the He-like F^{7+} beam in the post-stripping foil, long-lived metastable $1s2s\,{}^3S$ ions (277-μs lifetime) [28] were produced in addition to $1s^2\,{}^1S$ ground-state ions. Therefore the metastable beam fraction [28] had to be accounted for in the

cross-section analysis. The metastable beam fraction found in Ref. [28] increases gradually from about 5% for low-energy projectiles to about 30% for high-energy projectiles.

A tandem 45° parallel-plate electron spectrometer [29] with a channeltron detector was used to analyze the energy of all the collisionally produced electrons at zero degrees to the beam direction. Pressures of the target gases were varied from 2 mTorr for the lowest beam energy to 50 mTorr for the highest beam energy to maintain single collision conditions. Additional experimental details are provided in Refs. [29] and [30]. The absolute cross sections were obtained by normalizing the spectrometer efficiency to the binary encounter electron production calculated in the impulse approximation (IA) for 9.5 to 38-MeV $F^{9+}+H_2$ collisions [30].

III. DATA ANALYSIS

Shown in Fig. 1 are the measured total *KLL* Auger production cross sections as a function of projectile energy. Near the *KLL* resonance energy of 20 MeV, the RTE signature is clearly seen for H_2 targets. For He targets and for low projectile energies, the contribution due to electron capture by the $1s2s\ ^3S$ metastable beam component is predominant as expected. In Fig. 2 are shown selected electron spectra obtained at various projectile energies. The normalized double-differential yields are displayed after kinematically transforming to the projectile rest frame, and the background electrons arising mainly from binary encounter scattering have been subtracted. Normalized single-differential yields were extracted by fitting the observed lines with Lorentzian or Fano profiles folded with the response function of the electron spectrometer.

The $2s2p\ ^{3,1}P$ two-electron states (see Fig. 2) are attributed to $1s \rightarrow 2p$ excitation of the $1s2s\ ^3S$ metastable beam component [31]. In this paper we focus on the $1s2l2l'$ three-electron states produced by the *KLL* RTE process. The $1s2l2l'\ ^{(2S+1)}L$ doubly excited states can be produced from both incoming $1s^2\ ^1S$ and $1s2s\ ^3S$ states. The dominant production mechanisms are illustrated with their energy levels and spin configurations in Fig. 3.

It should be noted that RTE from $1s2s\ ^3S$ to $1s2l2l'\ ^{(2S+1)}L$ states is not energetically allowed. In addition, only those $1s2l2l'\ ^{(2S+1)}L$ states with appreciable Auger rates can be populated by RTE from the $1s^2\ ^1S$ state. NTE (nonresonant transfer excitation [32,33], in which a projectile electron is excited by the target nucleus) is possible from the $1s^2\ ^1S$ and $1s2s\ ^3S$ states and will be denoted hereafter as NTE1 and NTE2, respectively, for the sake of classification. Also shown in Fig. 3 is $2p$ capture (T) to the $1s2s\ ^3S$ beam component forming $1s2s2p\ ^{(2S+1)}L$ states. These states can also be formed from the $1s2s\ ^3S$ state by np capture followed by cascading to the $2p$ orbital. Capture to the $1s^2\ ^1S$ beam component does not form any doubly excited states.

In order to extract RTEA cross sections for each state, all the dominant contributions to the formation of each state, which are illustrated in Fig. 3, should be considered. The Auger electron count (Z), which is measured for one of the Auger states for an incoming number

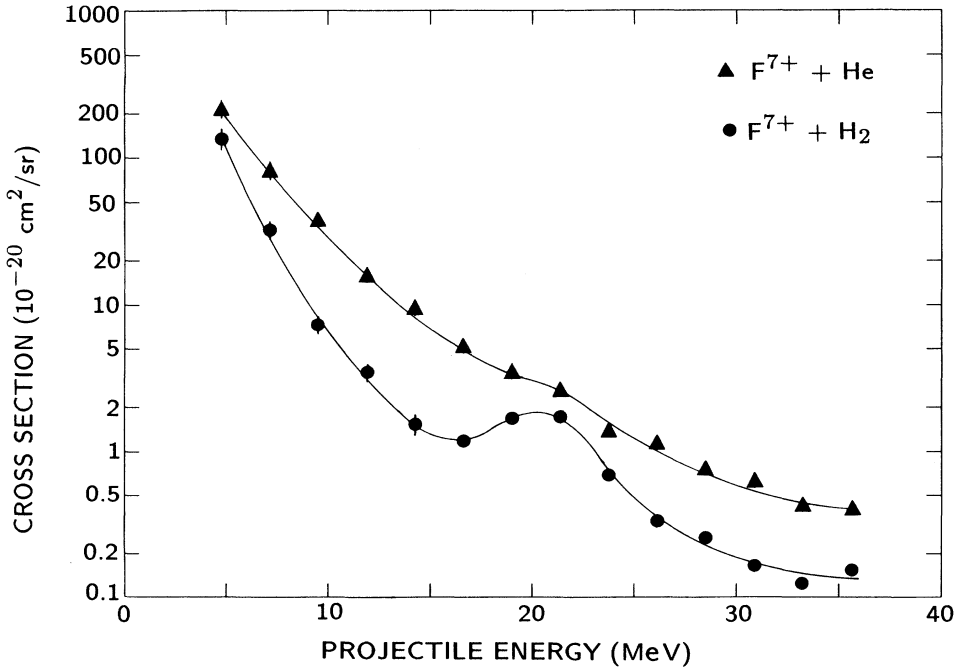

FIG. 1. Total *KLL* Auger production cross sections at zero degrees in collisions of F^{7+} with He and H_2 targets as a function of the projectile energy. The solid lines are drawn to guide the eye.

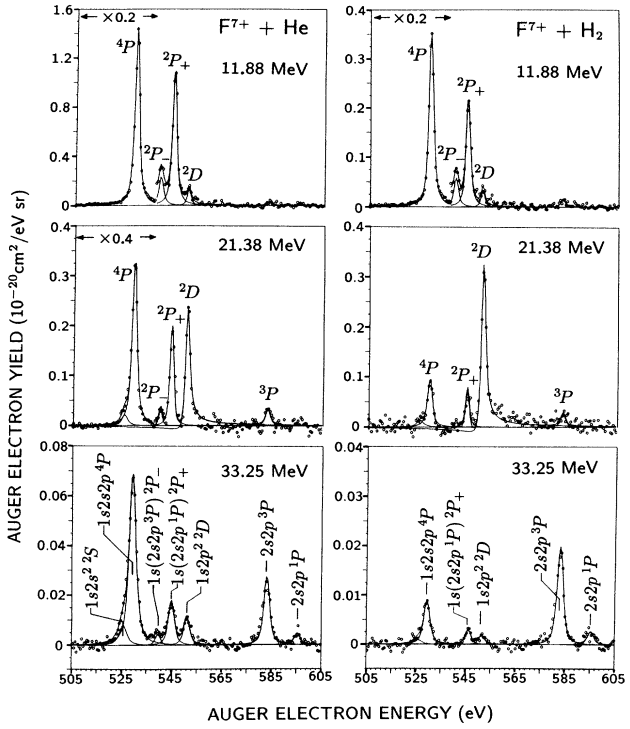

FIG. 2. Normalized zero-degree Auger-electron spectra (projectile rest frame) produced in $F^{7+}(1s^2\,{}^1S, 1s2s\,{}^3S)+He$ and H_2 collisions at three different projectile energies. Note the change of scale for the ^4P state in three of the spectra.

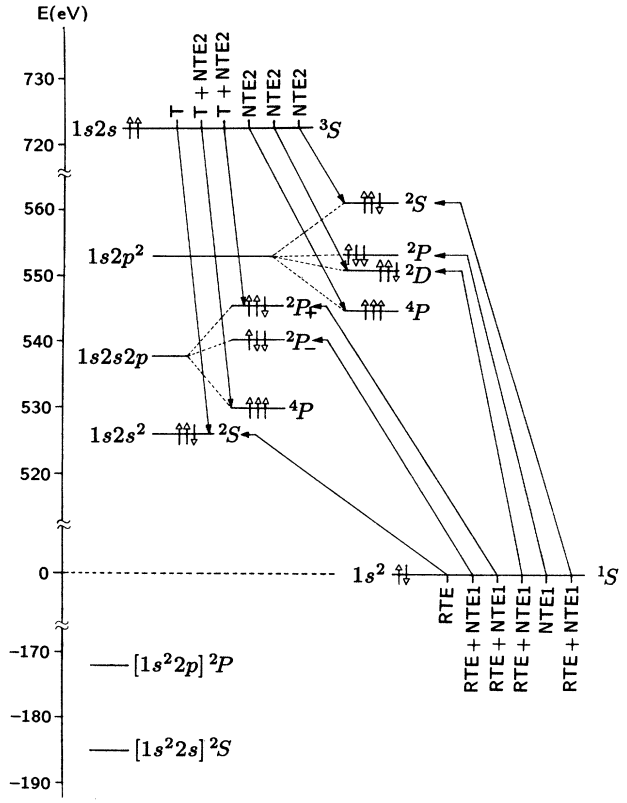

FIG. 3. Energy-level diagram with dominant mechanisms for the production of $1s2l2l'\,{}^{(2S+1)}L$ doubly excited states from $F^{7+}(1s^2\,{}^1S)$ ground state and $(1s2s\,{}^3S)$ metastable state.

(N_0) of F^{7+} projectiles, can be expressed as

$$Z=N_0F_g nl\left[\frac{d\sigma}{d\Omega}\right]_g\Delta\Omega\eta+N_0F_m nl\left[\frac{d\sigma}{d\Omega}\right]_m\Delta\Omega\eta\ , \quad (1)$$

where F_m and F_g are the metastable and ground-state beam fractions, respectively, $(d\sigma/d\Omega)_g$ and $(d\sigma/d\Omega)_m$ are the Auger production single-differential cross sections (SDCS) due to the ground-state and metastable beam components, respectively, n is target gas density, l is target gas length, $\Delta\Omega$ is the subtending solid angle of the electron spectrometer, and η is the spectrometer efficiency. The Auger production SCDS $(d\sigma/d\Omega)$ for each state is given by

$$\frac{d\sigma}{d\Omega}=\frac{Z}{N_0 nl\Delta\Omega\eta}\ , \quad (2)$$

which from Eq. (1) can be expressed as

$$\frac{d\sigma}{d\Omega}=F_g\left[\frac{d\sigma}{d\Omega}\right]_g+F_m\left[\frac{d\sigma}{d\Omega}\right]_m\ . \quad (3)$$

The data presented in Figs. 4 and 5 were evaluated using Eq. (2).

As seen in Fig. 3, the Auger SCDS $(d\sigma/d\Omega)_g$ is produced by RTEA or NTE1A, and in the same way the Auger SDCS $(d\sigma/d\Omega)_m$ is produced by TA or NTE2A. The "A" in the acronyms TA, NTE1A, and NTE2A refers to Auger decay following the processes of T (transfer), NTE1, and NTE2, respectively. Therefore, in general, the Auger production SDCS for each state can be given by

$$\frac{d\sigma}{d\Omega}=a\frac{d\sigma_{\rm RTEA}}{d\Omega}+b\frac{d\sigma_{\rm NTE1A}}{d\Omega}+c\frac{d\sigma_{\rm NTE2A}}{d\Omega}+d\frac{d\sigma_{\rm TA}}{d\Omega}\ , \quad (4)$$

where the coefficients a, b, c, and d are F_g, F_m, or 0 depending on the state production mechanism as shown in Fig. 3.

In the case of the ^2D and $^2P_+$ states, which show strong RTE signatures, the Auger production SCDS can be written using Eq. (4) and Fig. 3. For the ^2D state

$$\frac{d\sigma^D}{d\Omega}=F_g\left[\frac{d\sigma^D_{\rm RTEA}}{d\Omega}+\frac{d\sigma^D_{\rm NTE1A}}{d\Omega}\right]+F_m\frac{d\sigma^D_{\rm NTE2A}}{d\Omega}\ , \quad (5)$$

where the superscript D refers to the ^2D state. For the $^2P_+$ state

$$\frac{d\sigma^P}{d\Omega}=F_g\left[\frac{d\sigma^P_{\rm RTEA}}{d\Omega}+\frac{d\sigma^P_{\rm NTE1A}}{d\Omega}\right]+F_m\left[\frac{d\sigma^P_{\rm NTE2A}}{d\Omega}+\frac{d\sigma^P_{\rm TA}}{d\Omega}\right]\ , \quad (6)$$

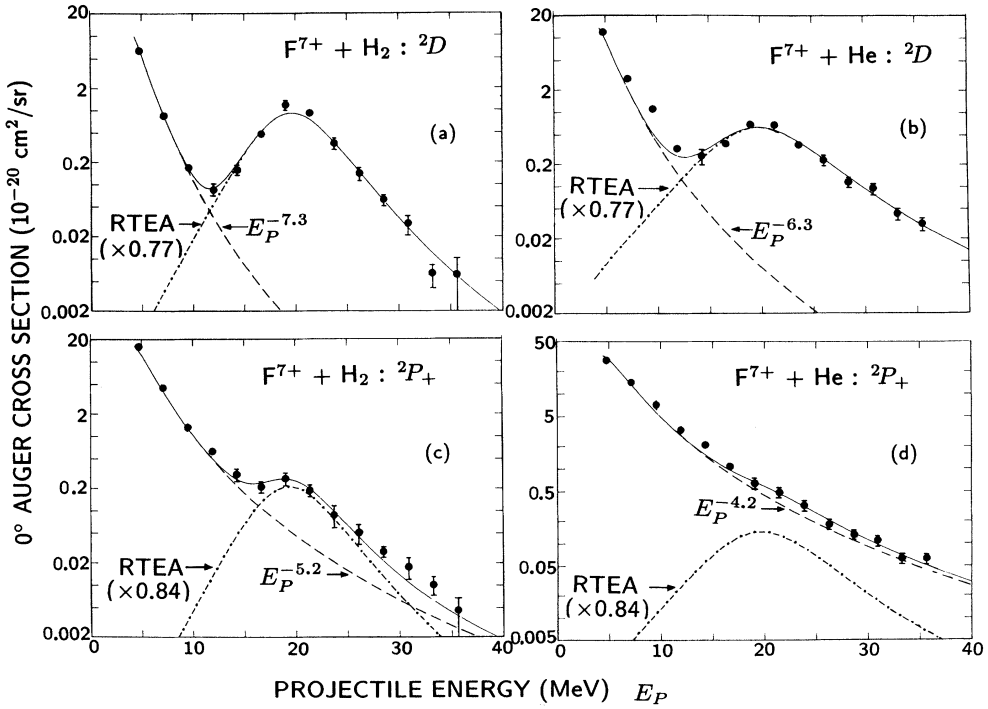

FIG. 4. Data points (●) represent the experimental absolute Auger electron production cross sections from $1s2p^2\,{}^2D$ and $1s(2s2p\,{}^1P)^2P_+$ states produced in $F^{7+}(1s^2\,{}^1S, 1s2s\,{}^3S)$+ He and H_2 collisions vs projectile energy. Solid lines in (a) and (b) are the sums of RTEA-IA (dot-dashed line) and NTE2A (broken line) contributions. Solid lines in (c) and (d) are the sums of RTEA-IA (dot-dashed line) and TA (dashed line) contributions.

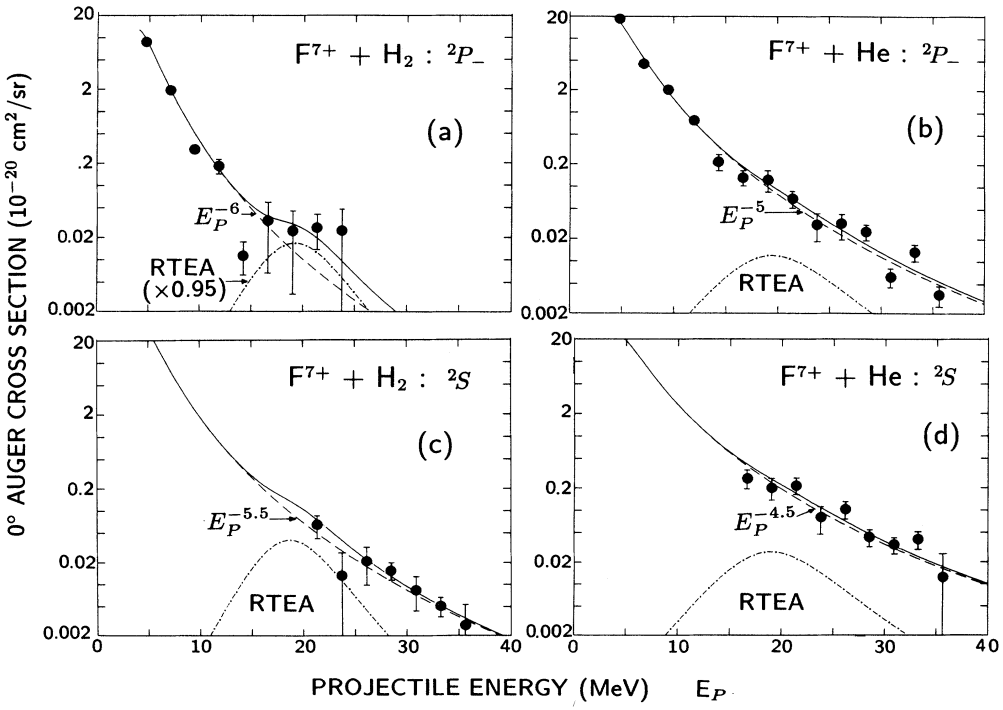

FIG. 5. Data points (●) represent the experimental absolute Auger-electron-production cross sections from $1s(2s2p\,{}^3P)^2P_-$ and $1s2s^2\,{}^2S$ states produced in $F^{7+}(1s^2\,{}^1S, 1s2s\,{}^3S)$+He and He_2 collisions vs projectile energy. Solid lines are the sums of RTEA-IA (dot-dashed line) and TA and/or NTE2A (dashed line) contributions.

where the superscript P refers to the $^2P_+$ state. All the contributing channels to Auger production, RTEA, NTE1A, NTE2A, and TA, are discussed and distinguished from each other as discussed below.

The absolute SDCS for Auger electron production from the $1s2p^2\,^2D$, $1s(2s2p\,^1P)^2P_+$, $1s(2s2p\,^3P)^2P_-$, and $1s2s^2\,^2S$ (hereafter denoted as ^2D, $^2P_+$, $^2P_-$, and ^2S states, respectively) are displayed in Figs. 4 and 5 as a function of projectile energy for both H_2 and He targets. As seen in Figs. 4 and 5, these states show strong, considerable, or weak RTE signatures depending on the state and target species. The theoretical curves in these figures will be discussed in Sec. V.

As seen in Fig. 2, the $1s2s2p\,^4P$ state is strongly populated for He targets and for low-energy projectiles. This state is formed primarily by $2p$ capture by the $1s2s\,^3S$ metastable beam [31,34]. The measured production cross sections for this state showed projectile energy E_P dependences of $E_P^{-(4.4\pm0.3)}$ and $E_P^{-(5.4\pm0.3)}$ for He and H_2 targets, respectively [31]. These energy dependences are reflected in the TA contribution to the other doubly excited states.

IV. IMPULSE APPROXIMATION

Although RTEA SDCS ($d\sigma_{\rm RTEA}/d\Omega$) can be treated within the usual impulse approximation [15] (IA), here we use a modified IA model that has already been used in the description of binary encounter electron (BEE) production [30]. Both BEE and RTE Auger electrons are produced as the result of quasielastic scattering with the same initial and final states, so that the same treatment of the IA can be applied. In addition, it has been shown that the $M_L=0$ substate is preferentially populated in RTE, and gives rise to an angular dependence in RTEA [11]. The modified IA model including this angular dependence yields the following expression for the RTEA SDCS [35]:

$$\frac{d\sigma^L_{\rm RTEA}}{d\Omega}=\frac{J(Q)}{V_P+Q}\frac{\Omega_{\rm RES}}{\varepsilon_0}|Y_{L0}|^2\,, \tag{7}$$

where

$$Q=\sqrt{2}(\sqrt{E_A+E_I}-\sqrt{t}\,)\,, \tag{8}$$

E_A is the Auger electron energy, E_I is the ionization potential of the target electron, $t=(m/M)E_p$ is the cusp energy, m/M is the electron-to-projectile-mass ratio, and V_P is the projectile velocity. All these values are in atomic units. $J(Q)$ is the Compton profile of the target electrons, and $\varepsilon_0=27.2126$ eV. Y_{L0} is a spherical harmonic and L refers to the angular momentum quantum number of the intermediate state ($|d\rangle$) of interest. For the present zero-degree RTEA measurement, the electron scattering angle is 180° in the projectile-rest frame. Thus Y_{L0} is evaluated at $\theta=180°$, and $|Y_{L0}(\theta=180°)|^2$ is simply $(2L+1)/4\pi$. $\Omega_{\rm RES}$ is defined [5,8] as

$$\Omega_{\rm RES}=\sigma_{\rm RES}\Delta E_{\rm bin}\,, \tag{9}$$

where the resonant excitation scattering cross section $\sigma_{\rm RES}=\xi\sigma_{\rm RC}$. $\sigma_{\rm RC}$ and ξ are the radiationless (or dielectronic) capture [5,8] (RC) cross section and the Auger yield of the $|d\rangle$ state, respectively. $\Delta E_{\rm bin}$ is the electron energy bin whose size is chosen to be much larger than the total width (transition rate) of the $|d\rangle$ state, which is $\Gamma^d=\Gamma^d_A+\Gamma^d_x$, Γ^d_A and Γ^d_x being the Auger and x-ray rate, respectively. $\Omega_{\rm RES}$ is invariant with $\Delta E_{\rm bin}$ and can be determined from the RTEA cross sections as far as the IA is valid. The interference effect between the Auger and binary-encounter electrons was neglected, since at $\theta_{\rm lab}=0°$ this effect was found to be less than 3% of RTEA cross sections [12].

The modified IA agrees somewhat better with the present experimental RTEA data than the standard IA in Ref. [15], particularly for the position of the RTEA resonance energy and on the low- and high-energy wings of the RTEA cross sections. These features are demonstrated in Fig. 6. This improved treatment is desirable for low-Z projectiles, where the IA starts to approach the limit of its validity. For example, it was found that only the present IA formalism could predict the RTEA resonance energy and result in a fair agreement with the resonance feature of the measured RTEA cross sections of Itoh *et al.* [4] for He^++He collisions [35].

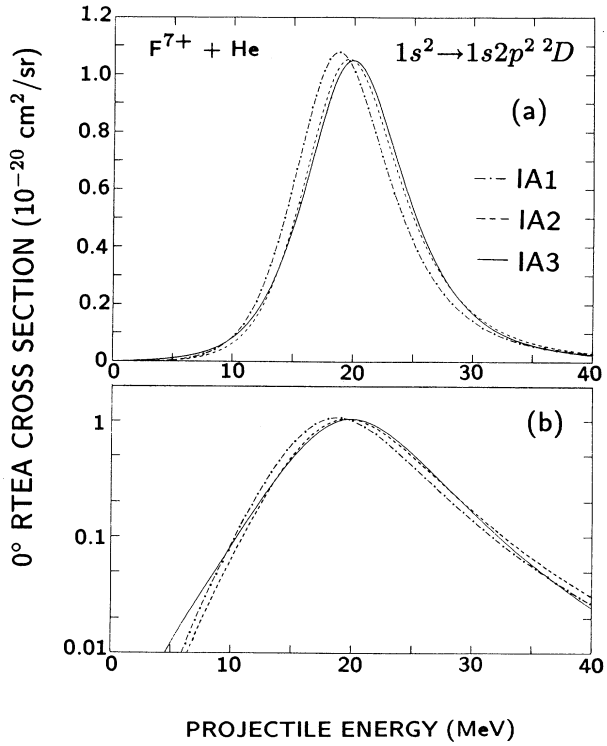

FIG. 6. Comparison [(a) in linear and (b) in log scale] of 0° RTEA for $1s2p^2\,^2D$ state for different impulse approximation treatment with He target. Dot-dashed line, Brandt [15] without target binding energy (24.5 eV) consideration; dashed line, Brandt [15] with target binding energy; and solid line, present [Eqs. (7) and (8)]. $\Omega_{\rm RES}=44.5\times10^{-19}$ cm^2 eV (see Table I) was used for all three RTEA calculations.

V. EXTRACTION OF RESONANT EXCITATION SCATTERING STRENGTHS

In the processes of NTE1 and NTE2, $1s \rightarrow 2p$ and $2s \rightarrow 2p$ excitations are involved, respectively. Since the $1s \rightarrow 2p$ excitation cross section is much smaller than the $2s \rightarrow 2p$ cross section, NTE1A makes a negligible contribution to the ^2D and $^2P_+$ Auger SDCS and may be neglected in Eqs. (5) and (6). The neglect of the NTE1A contribution is supported by previous measurements [12] where NTE1A cross sections were found to be at most a few percent of the maximum RTEA cross section for $1s2s2p^2\,^3D$ production in $F^{6+}(1s\,^2 2s)+H_2$ collisions.

Neglecting the NTE1A contribution, we were able to extract both the RTEA and NTE2A contributions to ^2D Auger production using Eq. (5). Here $\sigma^D_{\mathrm{NTE2A}}$ was taken to be proportional to $E_P^{-7.3}$ for H_2 and $E_P^{-6.3}$ for a He target. These E_P dependences were obtained from fits to the data shown in Figs. 4(a) and 4(b) and appear to be reasonable, when one considers that NTE is qualitatively proportional to the product of the excitation $(2s \rightarrow 2p)$ and single-capture cross sections. The sum of the RTEA and NTE2A contributions was fitted to the data and shown as solid lines in Figs. 4(a) and 4(b). In the case of a He target, a small NTE1A contribution may be present, but it does not affect extraction of the ^2D RTEA cross section. From the extracted ^2D RTEA cross section [see dot-dashed lines in Figs. 4(a) and 4(b)] and using the relationship between σ_{RTEA} and Ω_{RES} in Eq. (7), $\Omega_{\mathrm{RES}}(^2D)$ was found to be $(35\pm2)\times10^{-19}$ cm^2 eV for both H_2 and He targets.

In the extraction of the RTEA cross section for $^2P_+$ Auger production, a contribution, which comes from the TA process, must be accounted for as shown in Eq. (6). The TA contribution is dominant for the production of $^2P_+$ Auger electrons with He targets, as seen in Fig. 4(d), so no appreciable RTE signature was observed. However, in the case of a H_2 target, a significant RTE signature was present as seen in Fig. 4(c). This is expected when one considers that the $2p$ capture cross section with a H_2 target is much smaller than that with a He target [31], and that the H_2 Compton profile is narrower and higher than the He Compton profile [36]. The energy dependences for TA indicated by the broken line in Figs. 4(c) and 4(d) compared favorably with those found for the ^4P state (see Ref. [31]).

For a H_2 target, the NTE2A contribution to $^2P_+$ Auger SDCS is much smaller than the TA contribution. Therefore, neglecting both the NTE1A and NTE2A contributions and applying an $E_P^{-5.2}$ dependence for the TA contribution, the $^2P_+$ RTEA cross section was extracted using Eq. (6). The result is shown as a dot-dashed line in Fig. 4(c). Using Eq. (7), $\Omega_{\mathrm{RES}}(^2P_+)$ was determined to be $(14\pm2)\times10^{-19}$ cm^2 eV. With this value of $\Omega_{\mathrm{RES}}(^2P_+)$, the RTEA contribution is drawn in the case of a He target as shown in Fig. 4(d).

The Auger SDCS for the $^2P_-$ state showed a small RTE signature with a H_2 target as shown in Fig. 5(a), and Ω_{RES} was extracted and found to be $(1\pm0.3)\times10^{-19}$ cm^2 eV. As seen in Fig. 5(b) no appreciable RTE signature is observed for He targets due to the strong TA contribution. In the case of the $1s2s^2\,^2S$ state, a theoretical RTEA contribution is shown in Figs. 5(c) and 5(d), but no appreciable RTE signature could be observed experimentally.

Finally, we compare our measured Ω_{RES} with the theoretical values [11,12] given in the LS-coupling scheme (in cm^2 eV) by

$$\begin{aligned}\Omega_{\mathrm{RES}} &= \xi_d \Omega_{\mathrm{RC}} \\ &= \xi_d 2.475\times10^{-30} \\ &\quad\times \frac{(2L_d+1)(2S_d+1)}{(2L_i+1)(2S_i+1)} \frac{\Gamma_A(d\rightarrow i)}{E_A}\,, \end{aligned} \tag{10}$$

where $\xi_d = \Gamma^d_A/(\Gamma^d_A+\Gamma^d_x)$ is the Auger yield of the $|d\rangle$

TABLE I. Calculated and experimental resonance excitation scattering (RES) strengths (in units of 10^{-19} cm^2 eV) for the production of all $F^{6+}(1s2l2l')$ intermediate states. The initial and final states are $1s^2$ ground states. E_A and E_A^{expt} are theoretical (Refs. [37] and [38]) and measured Auger energies in eV. Γ_A and ξ are Auger rates (10^{13} s^{-1}) and Auger yields, respectively. Calculated radiationless capture (RC) strengths [5,8], related by $\Omega_{\mathrm{RC}} \equiv \Omega_{\mathrm{RES}}/\xi$, are also listed.

State	E_A	E_A^{expt}	Γ_A	ξ	Ω_{RC}	Ω_{RES}	$\Omega_{\mathrm{RES}}^{\mathrm{expt}}$
$1s2s^2\,^2S$	525.9	526.1	7.966[a]	0.9971[b]	7.50	7.48	
$1s2s2p\,^4P$	529.8	529.8	<0.001[c,e]	0.8947[c]	0.00	0.00	
$1s(2s2p\,^3P)^2P_-$	540.3	540.1	0.579[a,f]	0.694[b,g]	1.59	1.10	1.0±0.3
$1s(2s2p\,^1P)^2P_+$	545.6	545.2	6.184[a,f]	0.9896[b]	16.8	16.7	14±2
$1s(2p^2\,^3P)^4P$	544.9		~0.001[d]	0.9751[b]	0.01	0.01	
$1s(2p^2\,^1D)^2D$	551.1	551.2	10.13[a]	0.9785[b]	45.5	44.5	35±2
$1s(2p^2\,^3P)^2P$	553.1		0.0085[b]	0.0128[b]	0.02	0.00	
$1s(2p^2\,^1S)^2S$	561.2		1.23[b]	0.8574[b]	1.09	0.93	

[a]Reference [37].
[b]Auger rates and yields were evaluated from the values of the lifetimes τ and fluorescence yields ω given in Ref. [39].
[c]Reference [40].
[d]Reference [41].
[e]Auger rate of $1s2s2p\,^4P$ is about 10^{-5} of $1s(2s2p\,^1P)^2P_+$ Auger rate (see Ref. [42]).
[f]Auger rate in Ref. [42] is about 30% larger than this value from Ref. [37].
[g]Auger yield in Ref. [41] is about 10% smaller than this value from Ref. [39].

state, state $|i\rangle$ is the $1s^2\,{}^1S$ ground state, E_A is the Auger energy in eV, and L_d, S_d, L_i, and S_i represent the orbital and spin angular momentum quantum numbers of states $|d\rangle$ and $|i\rangle$, respectively. The RC and RES strengths from Eq. (10), E_A, Γ_A, and ξ for each $|d\rangle \rightarrow |i\rangle$ transition are listed in Table I along with our measured RES strengths.

As seen in Table I, theory predicts that only the ^2D and $^2P_+$ states have strong RES strengths. This is consistent with our experimental observation. Although the RES strengths of both ^2S states are expected to be appreciable, their RTEA SDCS are much smaller than those of the ^2D and $^2P_+$ states due to the angular factor $|Y_{L0}|^2$ in Eq. (7). Thus, no RTE signature for the $1s2s^2\,{}^2S$ state could be distinguished from the considerable TA contribution, and no measurable Auger line from $1s(2p^2\,{}^1S)^2S$ was observed above the background (binary encounter) electrons in the present work.

VI. CONCLUSION

In summary, a state-resolved *KLL* RTEA measurement of the formation of $F^{6+}(1s2l2l')$ states in (0.25–2)-MeV/u $F^{7+}(1s^2\,{}^1S, 1s2s\,{}^3S)$ collisions with He and H_2 has been performed. The measured RTEA SDCS at $\theta_{\rm lab}=0°$ were compared with the result of a modified RTEA-IA treatment leading to a good overall agreement. RES strengths for these states were extracted from the measured Auger SDCS using the modified IA formalism and compared with theoretical values and were found to be about 20% smaller than the theoretical values but within the experimental and theoretical uncertainties. This simultaneous agreement for both ^2D and $^2P_\pm$ states confirms that the $M_L=0$ magnetic substate is preferentially populated in RTE. As long as the IA is valid, RES strengths can be extracted from RTEA measurements. Therefore, 0° state-resolved RTEA measurements can complement dielectronic recombination measurements for any DR channel.

ACKNOWLEDGMENTS

This work was supported by the Division of Chemical Sciences, Office of Basic Energy Sciences, Office of Energy Research, U.S. Department of Energy. We would like to thank Professor C. D. Lin, Professor C. P. Bhalla, Professor J. H. McGuire, and Professor B. D. DePaola for helpful discussions.

*Present address: Department of Physics, University of Crete and Research Center of Crete, Iraklion, Greece.

†Present address: University of Frankfurt, Frankfurt, Germany.

‡Present address: Department of Physics, University of South Alabama, Mobile, AL 36688.

[1] J. A. Tanis, S. M. Shafroth, J. E. Willis, M. Clark, J. Swenson, E. N. Strait, and J. R. Mowat, Phys. Rev. Lett. **47**, 828 (1981); J. A. Tanis, E. M. Bernstein, W. G. Graham, M. Clark, S. M. Shafroth, B. M. Johnson, K. W. Jones, and M. Meron, *ibid.* **49**, 1325 (1982).

[2] For reviews on RTE see Ref. [3] and J. A. Tanis, E. M. Bernstein, C. S. Oglesby, W. G. Graham, M. W. Clark, R. H. McFarland, T. J. Morgan, M. P. Stöckli, K. H. Berkner, A. S. Schlachter, J. W. Stearns, B. M. Johnson, K. W. Jones, and M. Meron, Nucl. Instrum. Methods Phys. Res. B **10/11**, 128 (1985); E. M. Bernstein, M. W. Clark, J. A. Tanis, W. G. Graham, R. H. McFarland, T. J. Morgan, J. R. Mowat, D. W. Mueller, M. P. Stöckli, K. H. Berkner, R. J. McDonald, A. S. Schlachter, and J. W. Stearns, *ibid.* **24/25**, 232 (1987); R. Schuch, E. Justiniano, M. Schultz, P. H. Mokler, S. Reusch, S. Datz, P. F. Dittner, J. P. Giese, P. D. Miller, H. Schoene, T. Kambara, A. Müller, Z. Stachura, R. Vane, A. Warzcak, G. Wintermeyer, in *Proceedings of the XVI International Conference on the Physics of Electronic and Atomic Collisions, New York, 1989,* AIP Conf. Proc. No. 205, edited by A. Dalgarno, R. S. Freund, M. S. Lubell, and T. B. Lucatorto (AIP, New York, 1990), and references cited therein.

[3] Y. Hahn, Comments At. Mol. Phys. **19**, 99 (1987).

[4] A. Itoh, T. J. M. Zouros, D. Schneider, U. Stettner, W. Zeitz, and N. Stolterfoht, J. Phys. B **18**, 4581 (1985).

[5] J. K. Swenson, Y. Yamazaki, P. D. Miller, H. F. Krause, P. F. Dittner, P. L. Pepmiller, S. Datz, and N. Stolterfoht, Phys. Rev. Lett. **57**, 3042 (1986).

[6] T. J. M. Zouros, D. Schneider, and N. Stolterfoht, J. Phys. B **21**, L671 (1987).

[7] J. M. Anthony, S. M. Shafroth, M. Benhenni, E. N. Strait, T. J. M. Zouros, L. D. Hendrick, and D. M. Peterson, J. Phys (Paris) Colloq. **48**, C9-301 (1987).

[8] T. J. M. Zouros, D. H. Lee, S. L. Varghese, J. M. Sanders, J. L. Shinpaugh, P. Richard, K. R. Karim, and C. P. Bhalla, Phys. Rev. A **40**, 6246 (1989); Nucl. Instrum. Methods Phys. Res. B **40/41**, 17 (1989).

[9] B. D. DePaola, R. Parameswaran, and W. J. Axmann, Phys. Rev. A **41**, 6533 (1990).

[10] T. J. M. Zouros, D. Schneider, and N. Stolterfoht, Phys. Rev. A **35**, 1963 (1987).

[11] C. P. Bhalla, Phys. Rev. Lett. **64**, 1103 (1990).

[12] T. J. M. Zouros, C. P. Bhalla, D. H. Lee, and P. Richard, Phys. Rev. A **42**, 678 (1990).

[13] J. A. Tanis, E. M. Bernstein, W. G. Graham, M. P. Stöckli, M. Clark, R. H. McFarland, T. J. Morgan, K. H. Berkner, A. S. Schlachter, and J. W. Stearns, Phys. Rev. Lett. **49**, 2551 (1984); J. A. Tanis, E. M. Bernstein, M. W. Clark, W. G. Graham, R. H. McFarland, T. J. Morgan, B. M. Johnson, K. W. Jones, and M. Meron, Phys. Rev. A **31**, 4040 (1985); D. J. McLaughlin and Y. Hahn, Phys. Lett. A **112**, 389 (1985); W. G. Graham, E. M. Bernstein, M. W. Clark, J. A. Tanis, R. H. McFarland, T. J. Morgan, and A. Müller, Phys. Rev. A **33**, 3591 (1986); J. A. Tanis, E. M. Bernstein, M. W. Clark, W. G. Graham, R. H. McFarland, T. J. Morgan, J. R. Mowat, D. W. Mueller, A. Müller, M. P. Stöckli, K. H. Berkner, P. Gohli, R. J. McDonald, A. S. Schlachter, and J. W. Stearns, *ibid.* **34**, 2543 (1986); W. A. Schönfeldt, P. H. Mokler, D. H. H. Hoffmann, and A. Warzcak, Z. Phys. D **4**, 161 (1986); M. Schulz, E. Justiniano, R. Schuch, P. H. Mokler, and S. Reusch, Phys. Rev. Lett. **58**, 1734 (1987); S. Reusch, P. H.

Mokler, R. Schuch, E. Justiniano, M. Schulz, A. Müller, and Z. Stachura, Nucl. Instrum. Methods Phys. Res. B **23**, 137 (1987); R. Schuch, M. Schulz, E. Justiniano, H. Vogt, S. Reusch, and P. H. Mokler, *ibid.* **23**, 140 (1987); E. M. Bernstein, M. W. Clark, J. A. Tanis, W. G. Graham, R. H. McFarland, J. R. Mowat, D. W. Mueller, A. Müller, M. P. Stöckli, K. H. Berkner, R. J. McDonald, A. S. Schlachter, and J. W. Stearns, *ibid.* **23**, 154 (1987); D. J. McLaughlin and Y. Hahn, Phys. Rev. A **37**, 3587 (1988); **38**, 531 (1988); M. Schulz, R. Schuch, S. Datz, E. L. B. Justiniano, P. D. Miller, and H. Schöne, *ibid.* **38**, 5454 (1988); C. P. Bhalla and K. R. Karim, *ibid.* **39**, 6060 (1989); S. Datz, C. R. Vane, P. F. Dittner, J. P. Giese, J. G. del Campo, N. L. Jones, H. F. Krause, P. D. Miller, M. Schulz, H. Schöne, and T. M. Rosseel, Phys. Rev. Lett. **63**, 742 (1989).

[14] M. Schulz, J. P. Giese, J. K. Swenson, S. Datz, P. F. Dittner, H. F. Krause, H. Schöne, C. R. Vane, M. Benhenni, and S. M. Shafroth, Phys. Rev. Lett. **62**, 1738 (1989); J. K. Swenson, J. M. Anthony, M. Reed, M. Benhenni, S. M. Shafroth, D. M. Peterson, and L. D. Hendrik, Nucl. Instrum. Methods Phys. Res. B **24/25**, 184 (1987).

[15] D. Brandt, Phys. Rev. A **27**, 1314 (1983).

[16] Y. Hahn, Phys. Rev. A **40**, 2950 (1989).

[17] N. R. Badnell, Phys. Rev. A **41**, 3555 (1990).

[18] M. Benhenni, S. M. Shafroth, J. K. Swenson, M. Schulz, J. P. Giese, H. Schöne, C. R. Vane, P. F. Dittner, and S. Datz, Phys. Rev. Lett. **65**, 1849 (1990).

[19] J. M. Feagin, J. S. Briggs, and T. M. Reeves, J. Phys. B **17**, 1057 (1984).

[20] W. Fritsch and C. D. Lin, Phys. Rev. Lett. **61**, 690 (1988).

[21] A. M. Burgess, Astrophys. J. **141**, 1588 (1965); B. W. Shore, *ibid.* **158**, 1205 (1969); Y. Hahn, Adv. At. Mol. Phys. **21**, 123 (1985).

[22] P. F. Dittner, S. Datz, P. D. Miller, C. D. Moak, P. H. Stelson, C. Bottcher, W. B. Dress, G. D. Alton, and N. Nesković, Phys. Rev. Lett. **51**, 31 (1983).

[23] R. E. Marrs, M. A. Levine, D. A. Knapp, and J. R. Henderson, Phys. Rev. Lett. **60**, 1715 (1988).

[24] R. Ali, C. P. Bhalla, C. L. Cocke, and M. Stöckli, Phys. Rev. Lett. **64**, 633 (1990).

[25] P. G. Burke, Adv. At. Mol. Phys. **4**, 173 (1968); D. E. Golden, *ibid.* **14**, 1 (1978).

[26] For a recent review see N. Stolterfoht, in *Electron Correlation Processes in Energetic Ion-Atom Collisions,* edited by M. Ivascu, V. Florescu, and V. Zoran (World Scientific, Singapore, 1989), p. 342.

[27] M. L. Goldberger and K. M. Watson, *Collison Theory* (Wiley, New York, 1964); see Eqs. (11.60b) and (11.40).

[28] T. R. Dillingham, J. Newcomb, J. Hall, P. L. Pepmiller, and P. Richard, Phys. Rev. A **29**, 3029 (1984).

[29] D. H. Lee, T. J. M. Zouros, J. M. Sanders, J. L. Shinpaugh, T. N. Tipping, S. L. Varghese, B. D. DePaola, and P. Richard, Nucl. Instrum. Methods Phys. Res. B **40/41**, 1229 (1989).

[30] D. H. Lee, P. Richard, T. J. M. Zouros, J. M. Sanders, J. L. Shinpaugh, and H. Hidmi, Phys. Rev. A **41**, 4816 (1990).

[31] D. H. Lee, P. Richard, J. M. Sanders, T. J. M. Zouros, J. L. Shinpaugh, and S. L. Varghese, Nucl. Instrum. Methods Phys. Res. B **56/57**, 99 (1991).

[32] P. L. Pepmiller, P. Richard, J. Newcomb, T. R. Dillingham, J. M. Hall, T. J. Gray, and M. Stöckli, IEEE Trans. Nucl. Sci. **NS-30**, 1002 (1983).

[33] M. Clark, D. Brandt, J. K. Swenson, and S. M. Shafroth, Phys. Rev. Lett. **54**, 544 (1985).

[34] M. Terasawa, T. J. Gray, S. Hagmann, J. Hall, J. Newcomb, P. Pepmiller, and P. Richard, Phys. Rev. A **27**, 2868 (1983).

[35] D. H. Lee, Ph.D. thesis, Kansas State University, 1990.

[36] J. S. Lee, J. Chem. Phys. **66**, 4906 (1977).

[37] C. Can, T. W. Tunnell, and C. P. Bhalla, J. Electron Spectrosc. Relat. Phenom. **27**, 75 (1982).

[38] K. T. Chung and B. F. Davis (private communication).

[39] T. W. Tunnell, C. Can, and C. P. Bhalla, IEEE Trans. Nucl. Sci. **NS-26**, 1124 (1979).

[40] B. F. Davis and K. T. Chung, Phys. Rev. A **39**, 3942 (1989); **36**, 1948 (1987).

[41] E. Träbert, Nucl. Instrum. Methods Phys. Res. B **23**, 287 (1987).

[42] M. H. Chen and B. Crasemann, Phys. Rev. A **27**, 544 (1983).